Zero-Magnetic-Field Collective Insulator Phase in a Dilute 2D Electron System

V. M. Pudalov,[(1),(a)] M. D'Iorio,[(1)] S. V. Kravchenko,[(2),(a)] and J. W. Campbell[(3)]
[(1)] *National Research Council of Canada, Ottawa, Ontario, Canada K1A 0R6*
[(2)] *Physics Department, University of Nottingham, Nottingham, United Kingdom NG7 2RD*
[(3)] *University of Ottawa, Ottawa, Ontario, Canada K1N 6N5*

(Received 1 October 1992)

We report on a collective low temperature metal-insulator transition which develops in a dilute 2D electron system in Si at zero magnetic field, below a critical carrier density $n_{sc} \approx 10^{11}$ cm^{-2}. In the insulator phase, the dc conduction is thermally activated and exhibits a sharp threshold as a function of electric field. The collective insulator state at zero field shows many of the features attributed to the pinned Wigner solid. We have also observed a trend from a collective to a single-particle insulator state with decreasing electron density and/or increasing disorder.

PACS numbers: 73.40.Qv, 71.55.Jv, 71.30.+h

In the limit of zero temperature, the dilute two-dimensional electron (2DE) system is expected to become an insulator in the presence of disorder [1]. Various theoretical models for this insulating state have been proposed ranging from Anderson's single-particle localization (SPL) [1] to collective phases like the pinned Wigner solid (WS) [2], and the pinned charge density wave (CDW) [3]. Pioneering work [4] on low mobility Si samples revealed features indicative of a collective glassy state in high magnetic fields. The search for an electron ordered state in a quantizing magnetic field has recently led to the experimental observation of metal-insulator (MI) transitions in high mobility samples: GaAs-AlGaAs [5] heterostructures and Si-MOSFET's [6–8]. In these samples, reentrant MI transitions in a magnetic field were observed around fractional (mainly 1/5 in GaAs) and integer (1 and 2 in Si) filling factors. However, the realization of the "true" Wigner solid at zero magnetic field in GaAs would require an unrealistically dilute electron system since the critical density for quantum melting at $T = 0$ [9] (also known as "cold melting") is very low, i.e., $n_{cm} \sim 3 \times 10^8$ cm^{-2}. In contrast, the cold melting density in (100) Si should be at least 20× larger, due to the larger effective mass ($m^\star = 0.19 m_e$) and lower dielectric constant ($\kappa = 7.7$) which increases the ratio of the electron-electron interaction energy $[(\pi n_s)^{1/2} e^2/\kappa]$ to the kinetic energy ($\pi n_s h^2/2m^\star$) [8]. Therefore, a zero-field collective electron solid (ES) is more likely to be observed in high mobility Si inversion layers. There has not been, to our knowledge, any observation of the collective ES (and, in particular, the pinned Wigner solid) and its quantum melting at zero magnetic field in 2D. In our earlier work [6, 8], there is an indication, however, that the insulating phase does not disappear as $H \to 0$ but rather shifts to lower density and has features similar to those of the reentrant MI transitions in a magnetic field.

In this Letter, we present experimental evidence for the collective character of the low temperature metal-insulator transition at zero field in Si MOSFET's with weak disorder. The data show a trend from a collective to a single-particle insulator state with decreasing density and/or increasing disorder. We compare our data on nonlinear dc transport, activation energy, and threshold electric field with the available theoretical models and find best agreement with the pinned 2D Wigner solid.

Three samples with different peak mobilities, $\mu^{\rm peak}$, were measured: Si-5 with $\mu^{\rm peak} = 4.3 \times 10^4$ cm^2/V s, Si-11 with $\mu^{\rm peak} = 3.63 \times 10^4$ cm^2/V s, and Si-2 with $\mu^{\rm peak} = 2.42 \times 10^4$ cm^2/V s. The rectangular geometry of the samples is shown in the inset of Fig. 1(a) with a source to drain length $L = 5$ mm, a width of $w = 0.8$ mm, and an intercontact distance of $l = 1.25$ mm. The longitudinal resistance R_{xx} was measured using a four-probe technique with a differential electrometer and dc currents as low as 1 pA. Measurements were done in a dilution refrigerator in a temperature range 25–650 mK. A magnetic field below ≈ 100 G did not affect the results: by "*zero magnetic field*" we mean $H \leq 20$ G where the Landau levels are not resolved.

The experimental results are displayed in Figs. 1 and 2. Below a critical carrier density $n_{sc} \approx 10^{11}$ cm^{-2}, the longitudinal resistivity $\rho_{xx} = R_{xx} \times w/l$ exhibits insulating behavior, characterized by an exponential rise shown in Fig. 1(a) and a negative slope in the temperature dependence, $\partial R_{xx}/\partial T$. In the temperature range $\sim$ 80–650 mK, the temperature dependence of R_{xx} can be described by $R_{xx} \propto \exp(\Delta/kT)$ where the activation energy Δ drops linearly to zero at n_{sc}, as illustrated in Fig. 1(b). The critical carrier density is sample dependent, decreasing from 1×10^{11} cm^{-2} for Si-2 to 8×10^{10} cm^{-2} for Si-5 which is the highest mobility or least disordered sample. Concomitant with the appearance of these features in R_{xx}, the current-voltage characteristics exhibit a sharp drop in $\partial V/\partial I$ above a threshold electric field E_t as shown in Fig. 2(a). Over the entire range of densities, the threshold field decreases as $E_t \propto \delta n_s^k$ where $\delta n_s = (n_{sc} - n_s)$ and $k = 1.7$–1.8 [see Fig. 1(b)]. The dependencies of Δ and E_t on n_s are quite similar for all

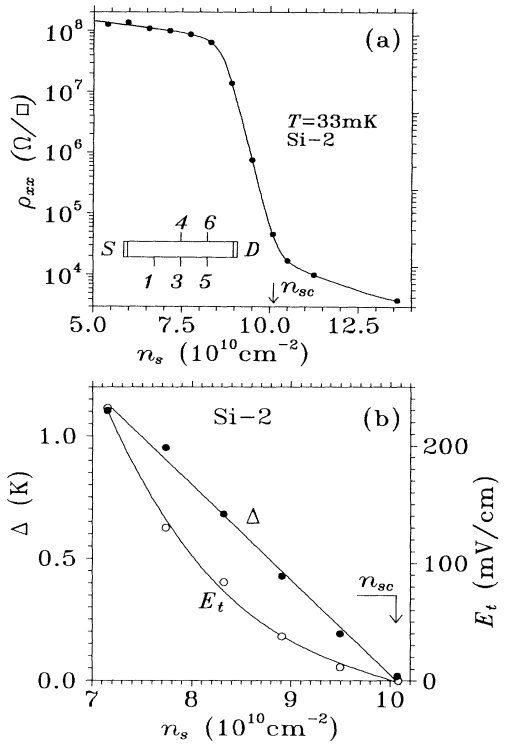

FIG. 1. (a) ρ_{xx} as a function of electron density in the activated regime. The inset shows the top view of the sample. (b) Activation energy and threshold electric field vs electron density.

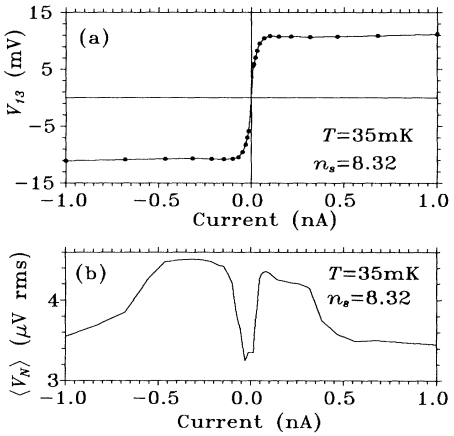

FIG. 2. (a) Typical threshold I-V characteristic. (b) Broad-band noise voltage measured between probes 1 and 3 as a function of source-drain current. n_s is in units of 10^{10} cm^{-2}.

three samples. The broad-band rms noise voltage $\langle V_N \rangle$ measured in a 1–300 kHz band using probes 1–3 exhibits a sharp rise as a function of current, coincident with the conduction threshold [see Fig. 2(b)].

Let us first consider the experimental results in the framework of single-particle localization. At the onset of the insulating phase, the longitudinal resistivity $\rho_{xx}(n_{sc})$ is of order $\simeq h/e^2 \simeq 3 \times 10^4\ \Omega$ which agrees qualitatively with the Anderson insulator [1] picture. Other results, however, suggest that the exponential growth of R_{xx} is not associated with single-particle localization in an electron gas: the capacitive measurements on Si-11 [7] do not show a decrease in the effective conducting area of the sample for $n_s \leq n_{sc}$, and the variable range hopping model [10] characteristic of SPL does not fit the conductivity above and below the threshold. In the SPL model, the conduction threshold is associated with a breakdown of localized states [11] which occurs when $eE_t\xi_0$ is comparable to the Fermi energy ϵ_F. An unreasonably high localization length ξ_0= 6 mm is required to account for the low threshold field at δn_s=0.1 $\times$ 10^{10} cm^{-2} and $\epsilon_F \simeq$ 6 K. A more accurate estimation on the basis of Ref. [11] yields a value of $E_t^{\rm SPL} = 2.9 \times 10^3$ V/cm which is 4 orders of magnitude higher than observed.

It is reasonable therefore to consider the transport data in the framework of the pinned WS or pinned CDW model. A detailed study of the activation energy shows that, at electric fields below threshold, the transport remains activated with $\Delta \propto (E_t - E)^\gamma$, where $\gamma \simeq 1$. Hence, both the temperature and the electric field affect one and the same transport mechanism and $|\partial\Delta(E)/\partial E| \sim \Delta(0)/E_t$. The derivative $\partial\Delta/e\partial E = \xi$ represents then a characteristic length scale. If transport below threshold is provided by point defect motion in the WS then $\xi \approx a \approx 200$ Å [12], where the lattice parameter $a = (\pi n_s)^{-1/2}$. The experimental values of ξ are $\sim 10^3$ times larger and, therefore, subthreshold transport is more likely provided by the motion of extended defects [13].

In the high electric field limit, the transport above threshold in the pinned WS or pinned CDW may be provided by the motion of depinned domains [14–16]. The evanescent threshold field at n_{sc} shown in Fig. 1(b) indicates that the transition at n_{sc} is not first order and is difficult to explain in the framework of strong pinning [14,15], when both the pinning force and correlation length are given by the impurities. In the weak pinning regime, the elastic theory of the CDW [16] predicts that $E_t = K_T a/2\pi e n_s L_D^2 = 0.19 \times 10^{-10}/L_D^2$ (V/cm) where $\kappa = 7.7$, K_T is the transverse shear modulus, and L_D is the correlation length (domain size) [3, 15, 16]. Using that formula and the experimental $E_t(n_s)$ data, we find that L_D diverges as $\propto (\delta n_s)^{-0.9}$ as plotted in Fig. 3. In the derivation of the formula for E_t, it was assumed [16] that the amplitude of the CDW, the pinning energy $(1/2)K_T a$, and the elastic modulus are fixed. In the vicinity of the second-order transition, all these parameters may, however, vanish. The critical exponent for L_D would then be 0.4 rather than 0.9 (see Fig. 3) if the pinning energy decays linearly like $\Delta(n_s)$.

The generated broad-band noise shown in Fig. 2(b) is appropriate for depinning of the CDW. For sliding do-

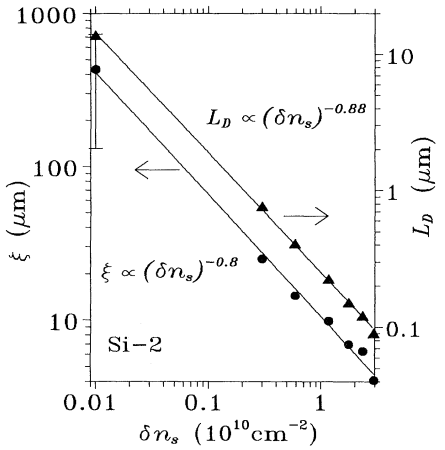

FIG. 3. Length scale in the vicinity of n_{sc}: $\xi = \partial\Delta/e\partial E$ for the subthreshold transport, and domain length L_D for the transport above threshold. Error bars when not shown are represented by the dot size.

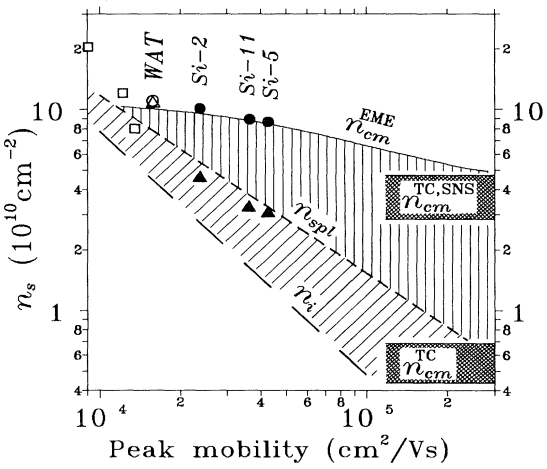

FIG. 4. Critical density vs sample peak mobility. The full circles designate the measured n_{sc} values; the hatched regions, n_{cm} calculated from Ref. [9] and Refs. [9, 21]. The full line represents $n_{cm}(n_i)$ calculated on the basis of Ref. [2]; the dashed lines, n_i and $n_{\rm spl}$ vs $\mu^{\rm peak}$ [17]. The full triangles indicate the $n_{\rm spl}$ evaluated from our data. The empty circle and triangle are taken from Ref. [4]. The empty squares denote the onset of activated transport from Ref. [18].

mains, one might expect narrow-band noise with frequency peaks related to the principal lattice parameters, or, at least, peaks on a broad-band background. In fact, preliminary data do show the presence of weak narrow-band noise with a current-dependent frequency spectrum.

In Fig. 3, the correlation length L_D drops with decreasing density [or increasing $\delta(n_s)$] thus driving the 2DE system towards single-particle localization. The SPL description is more appropriate when L_D is $\approx a$. We probed the role of disorder quantitatively by using Gold's calculation [17] for the mobility of Si(100) inversion layers. It yields a satisfactory description of $\mu^{\rm peak}$ vs n_s for our samples. The results of Ref. [17] are used to relate $\mu^{\rm peak}$ to the density of impurities n_i, which is a more appropriate measure of disorder since the impurities are the major source of electron scattering at low n_s [1] (below 2×10^{11} cm^{-2} for our samples). The long dashed line in Fig. 4 shows n_i vs $\mu^{\rm peak}$. The empty squares depict the experimental data [18] for the Anderson transition. The boundary for SPL, denoted $n_{\rm spl}$, is estimated from n_i and depicted by a short dashed line. Theoretical calculations of n_i and $n_{\rm spl}$ [17] have been done specifically to fit the data for low mobility samples assuming an average magnitude of the surface roughness $\delta = 3.7$ Å and a correlation length $\Lambda = 15$ Å. For our high mobility samples where $\delta < 3.7$ Å and $\Lambda \gg 15$ Å [19], we conclude that the interface roughness scattering is lower and that the calculated short-dashed line is *the highest estimate* of $n_{\rm spl}$ in our samples. The n_{sc} values for the three samples, indicated by the full circles in Fig. 4, are at least $2\times$ higher than the $n_{\rm spl}$ values. This agrees with the collective character of the transition at n_{sc}.

We were unable to make direct R_{xx} measurements down to $n_s \sim n_{\rm spl} \approx 1 \times 10^{10}$ cm^{-2} due to a rapid increase in the probe resistance, but, in order to examine the validity of our interpretation, we extrapolated the domain length L_D to lower n_s. The resulting estimates of $n_{\rm spl}$ corresponding to the criterion $L_D = 2a$ are indicated by full triangles in Fig. 4. The "WAT" empty circle and the triangle designate respectively the onset of the insulating phase and the estimated $n_{\rm spl}$ (using the same criterion), from cyclotron resonance data by Wilson, Allen, and Tsui [4]. We interpret the lower dashed region as the estimated crossover to SPL and obtain reasonable agreement with all the data plotted in Fig. 4. The vertically dashed region designates then a collective insulator phase, confined between the metallic state above the n_{cm} boundary and presumably the Anderson insulator below the $n_{\rm spl}$ line.

The plot includes an estimated quantum melting density for the ideal WS: $n_{cm}^{\rm TC} = (0.43\text{–}0.7) \times 10^{10}$ cm^{-2} from Ref. [9] using the appropriate $m^\star$ and κ for the Si-SiO_2 interface. It is lower than the critical carrier density data plotted in Fig. 4. Models which can remove this discrepancy include the paired electron crystal [20] with a lower ground-state energy than the regular monoelectronic WS [9], and the enhanced WS in coupled electron layers [21] with $n_{sc} \simeq 7 \times n_{cm}^{\rm TC}$ [if it can be extended to the two valley system in (100) Si [8]]. This latter estimation $n_{cm}^{\rm TC,SNS} = (2.9\text{–}4.8) \times 10^{10}$ cm^{-2} is plotted in Fig. 4 and agrees with our data.

It is known that weak disorder can stabilize the WS due to the creation of a gap in the phonon spectrum and hence a limited zero point displacement [2]. We calculated the mean square displacement (MSD) of the pinned WS at $T = 0$ for given n_i values as the area under the

phonon spectral density of the pinned WS for the relative strength of the pinning potential $\lambda = 1$ [2]. From the MSD as a function of the density of impurities, we obtain the cold melting density dependence on n_i assuming that, for the ideal WS, n_{cm} tends to $n_{cm}^{\mathrm{TC,SNS}}$ as $n_i \to 0$. The result has no fitting parameters and is shown in Fig. 4 as a full line n_{cm}^{EME}; the agreement with the data seems quite good. The full line merges with the dashed SPL boundary at $\mu^{\mathrm{peak}} \simeq 12 \times 10^3$ cm^2/Vs which accounts for the lack of collective MI transitions in poorer mobility Si samples.

In summary, our data on nonlinear dc transport in the vicinity of the low temperature metal-insulator transition at $H = 0$ in high mobility Si MOSFET's strongly support the collective character of that transition. As the electron density is decreased or the disorder is increased, the collective insulator state is driven into a single-particle one. The collective insulator state at $H = 0$ shares many of the features of the pinned Wigner solid. The measured critical density of the MI transition as a function of disorder is consistent with quantum melting of the pinned Wigner solid.

After the completion of this work we learned that a transition from a polarized WS to a partially polarized liquid was recently calculated at $r_s \approx 10$ (i.e., at $n_{sc} = 13.7 \times n_{cm}^{\mathrm{TC}}$) taking into account numerically the disorder in our Si samples [22]. This agrees within 15% accuracy with the data shown in Fig. 4.

We wish to thank S.-T. Chui for stimulating discussions and Donald Brown for his expert technical assistance.

[a] Permanent address: Institute for High Pressure Physics, Troitsk, 142092, Moscow district, Russia.

[1] For a review see T. Ando, A. B. Fowler, and F. Stern, Rev. Mod. Phys. **54**, 437 (1982).
[2] A. C. Eguiluz, A. A. Maradudin, and R. J. Elliott, Phys. Rev. B **27**, 4933 (1983).
[3] H. Fukuyama and P. A. Lee, Phys. Rev. B **17**, 535 (1978).
[4] S. Kawaji and J. Wakabayashi, Solid State Commun. **22**, 87 (1977); B. A. Wilson, S. J. Allen, and D. C. Tsui, Phys. Rev. B **24**, 5887 (1981).
[5] E. Y. Andrei, G. Deville, D. C. Glattli, F. I. B. Williams, E. Paris, and B. Etienne, Phys. Rev. Lett. **60**, 2765 (1988); V. J. Goldman, M. Santos, M. Shayegan, and J. E. Cunningham, Phys. Rev. Lett. **65**, 2189 (1990); H. W. Jiang, R. L. Willett, H. L. Stormer, D. C. Tsui, L. N. Pfeiffer, and K. W. West, Phys. Rev. Lett. **65**, 633 (1990).
[6] M. D'Iorio, V. M. Pudalov, and S. G. Semenchinsky, Phys. Lett. A **150**, 422 (1990).
[7] S. V. Kravchenko, J. A. A. J. Perenboom, and V. M. Pudalov, Phys. Rev. B **44**, 13 513 (1991).
[8] M. D'Iorio, V. M. Pudalov, and S. G. Semenchinsky, Phys. Rev. B **46**, 15992 (1992); S. V. Kravchenko, V. M. Pudalov, J. Campbell, and M. D'Iorio, Pis'ma Zh. Eksp. Teor. Fiz. **54**, 528 (1991) [JETP Lett. **54**, 532 (1991)].
[9] B. Tanatar and D. M. Ceperley, Phys. Rev. B **39**, 5005 (1989).
[10] B. I. Shklovskii and A. L. Efros, *Electronic Properties of Doped Semiconductors*, edited by M. Cardona, Springer Series in Solid State Sciences Vol. 45 (Springer-Verlag, Berlin, 1984).
[11] Y. C. Lee, C. S. Chu, and E. Castano, Phys. Rev. B **27**, 6136 (1983).
[12] B. I. Shklovskii (private communication).
[13] S. T. Chui and K. Esfarjani, Phys. Rev. Lett. **66**, 652 (1991).
[14] I. M. Ruzin, S. Marianer, and B. I. Shklovskii, Phys. Rev. B **46**, 3999 (1992).
[15] P. A. Lee and T. M. Rice, Phys. Rev. B **19**, 3970 (1979).
[16] B. G. A. Normand, P. B. Littlewood, and A. J. Millis, Phys. Rev. B **46**, 3920 (1992).
[17] A. Gold, Phys. Rev. Lett. **54**, 1079 (1985); A. Gold and W. Gotze, Phys. Rev. B **33**, 2495 (1986).
[18] A. Yagi and M. Nakai, Surf. Sci. **98**, 174 (1980).
[19] M. S. Khaikin, A. M. Troyanovskii, V. S. Edelman, V. M. Pudalov, and S. G. Semenchinskii, Pis'ma Zh. Eksp. Teor. Fiz. **44**, 193 (1986) [JETP Lett. **44**, 245 (1986)].
[20] K. Moulopoulos and N. W. Ashcroft, Phys. Rev. Lett. **69**, 2555 (1992).
[21] L. Swierkowski, D. Neilson, and J. Szymanski, Phys. Rev. Lett. **67**, 240 (1991).
[22] S.-T. Chui and B. Tanatar (to be published).